Separation Science and Technology
Publication details, including instructions for authors and subscription information:
http://www.informaworld.com/smpp/title~content=t713708471

Synthesis and Characterization of Zeolite Based Porous Ceramic Membranes

R. Roque-Malherbe[a]; W. del Valle[a]; F. Marquez[a]; J. Duconge[a]; M. F. A. Goosen[a]
[a] School of Science and Technology, University of Turabo, Gurabo, PR, USA

To cite this Article Roque-Malherbe, R. , Valle, W. del , Marquez, F. , Duconge, J. and Goosen, M. F. A.(2006) 'Synthesis and Characterization of Zeolite Based Porous Ceramic Membranes', Separation Science and Technology, 41: 1, 73 — 96
To link to this Article: DOI: 10.1080/01496390500446277
URL: http://dx.doi.org/10.1080/01496390500446277

Separation Science and Technology, 41: 73–96, 2006

ISSN 0149-6395 print/1520-5754 online
DOI: 10.1080/01496390500446277

Synthesis and Characterization of Zeolite Based Porous Ceramic Membranes

R. Roque-Malherbe, W. del Valle, F. Marquez, J. Duconge, and M. F. A. Goosen
School of Science and Technology, University of Turabo, Gurabo, PR, USA

Abstract: New porous zeolite based membranes were synthesized using a ceramic methodology and characterized by means of XRD, SEM, EDAX and permeation tests. The membranes were produced by thermal transformation of natural clinoptilolite. The XRD study showed clinoptilolite amorphization at 600–900°C. A posterior recrystallization to a siliceous phase and a compact aluminosilicate phase at 900–1150°C was also produced. The Permeability [B] and Permeance [Π] of H_2 and CO_2 were measured using the Darcy Law correlation. It was also applied for gaseous laminar flow using the Carman-Kozeny equation. With the help of this equation the membrane pores sizes were measured. It was shown that the membrane porosity can be controlled by the grain size of the original natural zeolite powder. The membranes were further transformed by hydrothermal synthesis to obtain materials covered with an $AlPO_4$-5 molecular sieve. In conclusion, novel, inexpensive, strong, high permeation rate, and high temperature membranes were produced with natural clinoptilolite, a low cost and available material.

Keywords: Zeolite based ceramic membranes, clinoptilolite, hydrothermal synthesis

INTRODUCTION

Membranes have been employed for the treatment of a variety of fluids ranging from gases, waste water, seawater, milk, yeast suspensions as well

Received 9 May 2005, Accepted 20 October 2005
Address correspondence to Prof. Dr. R. Roque-Malherbe, School of Science and Technology, University of Turabo, PO Box 3030, Gurabo, PR 00778-3030, USA. E-mail: rroque@suagm.edu

as other fluids (1–11). A membrane is a perm-selective barrier between two phases capable of being permeated due to a driving force, such as pressure, concentration or electric field gradient (4, 5) (see the appendix for a description of transport mechanisms in porous membranes). From the point of view of the material, membranes are categorized as organic or inorganic. In our case we will be focusing on inorganic membranes. These membranes are classified as, porous and microporous and symmetric and asymmetric (2, 4, 5). Porous membranes are those with pores in the mesoporous (2–50 nm) and macroporous (greater than 50 nm) domain. Microporous membranes are those with pore diameters between 0.3–2 nm (4). Porous and microporous inorganic membranes are made of alumina, silica, carbon, zeolites, and other materials (3). They are generally prepared by the slip coating method, ceramic technique, and sol-gel method (3–5). Inorganic membranes are employed in gas separation (3–5), catalytic reactors (2, 7), gasification of coal (3), water decomposition (3) and other applications (8, 9, 11).

The materials used for inorganic porous membrane synthesis experience phase transformations, structural changes and sinterization at high temperature (3, 6). As a result, the maximum temperature at which porous inorganic membranes could be used is 400–1000°C (3).

Porous membranes are used in microfiltration, ultrafiltration (4, 5) and supports for microporous material layer (3), such as a zeolite thin film (8). Also, porous membranes are used as a support for the synthesis of asymmetric membranes with a dense thin film (2, 7).

The mechanical strength of self-supported microporous inorganic membranes is normally inadequate (3, 8). Consequently, mechanically robust porous substrates are used as supports. The macro and/or mesopores of the support are covered with films of a micropore material. The porous support gives mechanical stability while the zeolite is intended to carry out selective separations (3, 8). Different methods have been used to deposit microporous thin films, specifically, including sol-gel, pyrolysis and deposition techniques (2, 3).

The synthesis and characterization of permselective inorganic membranes is a flourishing activity in materials science (1, 7). However, for the commercial exploitation of these membranes much work remains to be done (7). It is necessary to increase the membrane permeance to resolve the brittleness problems, to be able to scale up the process and to increase the membrane area per unit volume (7). It is also necessary to understand and model the process of gas transport through porous (2, 4, 5, 12, 13) and microporous (9, 12, 14–16) membranes.

It was previously shown (17) that if a natural zeolite, specifically a clinoptilolite, is thermally treated, at temperatures higher than 500°C, after dehydration, a phase transformation occurs of the original natural clinoptilolite to a practically amorphous phase (600–900°C). Recrystallization then occurs to a crystalline silica and a compact aluminosilicate phase (900–1150°C) (Fig. 1). It was also shown that if a ceramic methodology is

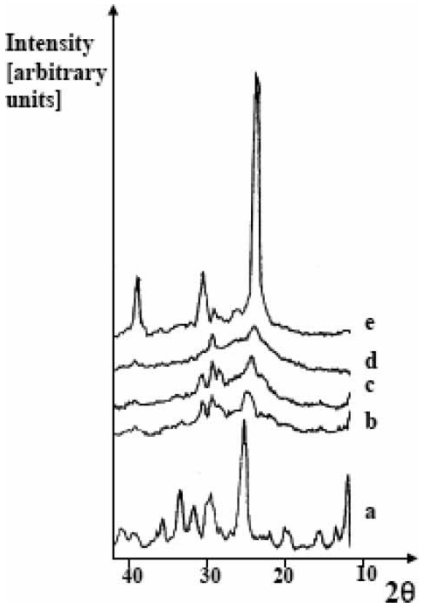

Figure 1. X-ray diffraction patterns (arbitrary units vs 2θ) of a natural clinoptilolite (a) and clinoptilolite wafers sintered at 600°C, (b) 800°C, (c) 900°C (d) and 1100°C (e) (17).

applied, that is to say, if the zeolite is ground and the powders obtained are sieved to particles of grain size of 50–100 μm, and if wafers are prepared with these fine particles by pressing at 100 MPa, and the wafers are thermally treated at 500, 600, 700, 900, 1000, and 1150°C, an increase is observed in the density of the ceramic membrane from 1.4 g/cm^3 at room temperature to 2.2 g/cm^3 at 1150°C (17) (Fig. 2). This means that by applying the ceramic method, materials are obtained which possess good mechanical properties (17, 18) and are porous.

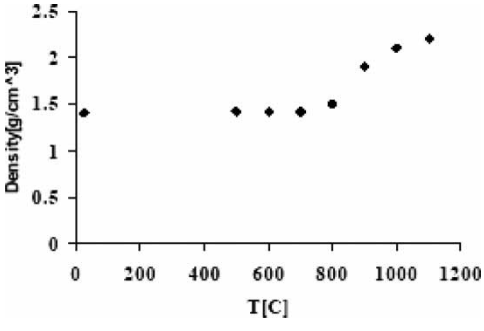

Figure 2. Wafer density [g/cm^3] versus temperature [°C] (17).

One of the major challenges is the development of inorganic membranes which are (7)

i. inexpensive
ii. not brittle
iii. have acceptable high temperature permeation rates
iv. reproducible at large scale

The aim of the present research was to synthesize new porous, not-brittle, with significant permeation rate membranes, by means of a ceramic methodology, using as raw material an available material, i.e., natural clinoptilolite. These membranes were characterized applying XRD, SEM, EDAX and permeation tests, to show that they can be used as filters and also as supports for the preparation of composite membranes covered with a microporous $AlPO_4$-5 molecular sieve, to increase it's selectivity.

EXPERIMENTAL

Materials

The analyzed natural zeolite (sample CSW) was mined in Sweetwater, Wyoming, USA. The sample was provided by ZeoponiX Inc., Louisville, CO, USA. The mineralogical phase composition of sample CSW was calculated, using a previously developed methodology (18), by means of standards, that is, two very well-characterized samples, the clinoptilolite samples, labeled HC and GR, whose mineralogical composition are reported in Table 1 (Fig. 3). The measured composition was 90 ± 5 wt.% clinoptilolite and 10 ± 5 wt.% of montmorillonite (2–10 wt.%), quartz (1–5 wt.%), calcite (1–6 wt.%), feldspars (0–1 wt.%), magnetite (0–1 wt.%) and volcanic glass (3–6 wt.%).

Table 1. Mineralogical composition (in wt.%) of a pair of natural clinoptilolite samples adopted in the present study as standards (18,24)

Sample	Clinoptilolite	Others
HC	85	15
GR	85	15

Note: Others: Montmorillonite (2–10 wt.%), quartz (1–5 wt.%), calcite (1–6 wt.%), feldspars (0–1 wt.%), magnetite (0–1 wt.%) and volcanic glass (3–6 wt.%).

The error in the mineralogical composition is $\pm 5\%$.

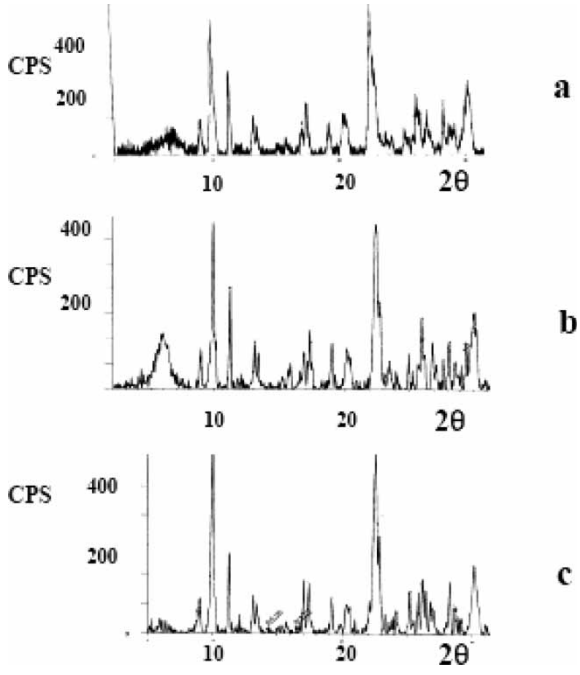

Figure 3. X-ray diffraction profiles (counts per second (CPS) versus 2θ) of CSW; (a) GR (b) HC (c) samples.

All the consumed chemicals were of analytical grade. The source materials for the synthesis were: deionized water, orthophosphoric acid (Merck, 85 wt.% H_3PO_4) triethylamine (TriEA), (Riedel de Haen, $(C_2H_5)_3N$), aluminum triisopropylate (Merck, $Al(C_3H_7O)_3$) hydrofluoric acid (Merck, 40 wt.% HF in water). The salt solutions used for the zeolite ionic exchange were prepared with NaCl and NH_4Cl provided by Fisher. The gases utilized in the single gas permeation test study were pure H_2 and CO_2 (99.99%) provided by Praxair.

Hydrothermal Synthesis

For the synthesis of the $AlPO_4$-5-zeolite based porous membrane composite the "in-situ" membrane growth technique (8) was chosen. The support, i.e., the zeolite based porous ceramic membrane is put in contact with the synthesis mixture and then subjected to a hydrothermal synthesis process. The batch preparation was as follows (19):

i. 7 g H_2O + 3.84 g of H_3PO_4, mix
ii. (i) + 2.07 g $(C_2H_5)_3N$, add $(C_2H_5)_3N$ dropwise and mix

iii. (ii) + 5.23 g $Al(C_3H_7O)_3$, add in small amounts at 0°C with intense stirring then stir the mixture at room temperature for 2 hours
iv. 0.83 g HF + 89.2 g H_2O, mix
v. [(iii) + (iv)], stir for 2 h

Then the gel was poured on the membrane in a 150 ml Teflon-lined steel autoclave and was treated for 24, 48, and 72 hours at 180°C without agitation.

METHODS

X-ray Diffraction (XRD), Scanning Electron Microscopy (SEM), and Energy Dispersive Analysis (EDAX)

The X-ray diffractograms were obtained in a Siemmens D5000 X-ray Diffractometer, in vertical set up: θ–2θ geometry. With Cu-K_α radiation source, Ni filter and Graphite monochromator.

The SEM and EDAX studies were carried out, with a JEOL Model 5800LV electron microscope with an Energy Dispersive X-ray Analysis accessory, EDAX-DX-4, to perform the elemental chemical analysis of the sample. The acceleration of the electron beam was 20 kV. The sample grains ($\phi \approx 3$ mm) were glued with silver colloid to the sample-holder and were coated at vacuum by cathode sputtering with a 30–40 nm gold film prior to observation.

Cationic Composition and Si/Al Relation of the Natural Clinoptilolite

The experimental evaluation of the cationic composition of the CSW sample was carried out as follows (20): 1 g of the natural zeolite sample CSW was refluxed at 373 K for 6 h in 1 liter of a 2 M solution of NH_4Cl to produce a homoionic sample NH_4-CSW. The degree of exchange of Na^+, K^+, Ca^{2+} and Mg^{2+} was measured using Atomic Absorption spectrometry (Perkin Elmer 3300 AA spectrometer) (Table 2). The CSW sample was additionally studied by EDAX. However, this study was carried out with a sample in the homoinic form of

Table 2. Cationic composition of the natural clinoptilolite sample CSW

Sample	Na^+ [mequiv/g]	K^+ [mequiv/g]	Ca^{2+} [mequiv/g]	Mg^{2+} [mequiv/g]
CSW	1.24	0.21	0.49	0.09

Note: The error in the Na^+, K^+, Ca^{2+} and Mg^{2+} cationic composition is ± 0.02 mequiv/g and the error in TCEC is ± 0.1 mequiv/g.

Table 3. Chemical composition (in wt.%) of the Na-CSW sample, determined by energy dispersive X-ray analysis in a JEOL model 5800LV scanning electron microscope

Sample	O	Si	Al	Fe	Ca	Mg	Na	K
Na-CSW	45.25	37.48	9.25	1.06	0.05	0.58	5.46	0.90

the natural zeolite, that is, sample CSW was refluxed (at 373 K) five times, for 4 h each period, in a 2 molar solution of NaCl to produce sample Na-CSW. The results of the EDAX study of sample Na-CSW are reported in Table 3. Consequently, the silicon aluminum rate of sample CSW was $Si/Al = 4.1$.

Ceramic Technique

The natural CSW sample was ground with a Bel-Art Products Micro-Mill® mechanic grinding machine. The powders obtained were sieved using the following sieves: greater than 100 mesh, 100–50 mesh, 50–40 mesh and 40–30 mesh to obtain particles of average grain diameter (d_p) of 50–100, 220, 340 and 500 μm respectively (Table 4). Cylindrical wafers (12.7 mm diameter and of 3 ± 0.1 mm height) were prepared by pressing at 250 MPa with a Carver Manual Hydraulic Press Model 3912, 0.55 ± 0.01 g of the zeolite powder. The wafers were thermally treated in a Fisher Scientific, Isotemp® Muffle Furnace 650 Series at 500, 600, 700, 900, 1000, and 1100°C during 1 and 2 hours with a heating rate of 40°C/min and a cooling rate of 1°C, to obtain the zeolite based ceramic membranes. SEM micrographs of sintered ceramic materials are shown in Fig. 4a, 4b (17) and Fig. 4c.

Permeation Test Facility

Single gas pure H_2 or pure CO_2, permeation tests were carried out in a permeation test facility (Fig. 5a) consisting of stainless steel tubing, valves,

Table 4. Average particle size of the clinoptilolite powders used for porous membrane synthesis

Clinoptilolite particle classification [mesh]	Average particle diameter d_p [μm]
Greater than 100	50–100
100–50	220
50–40	340
40–30	500

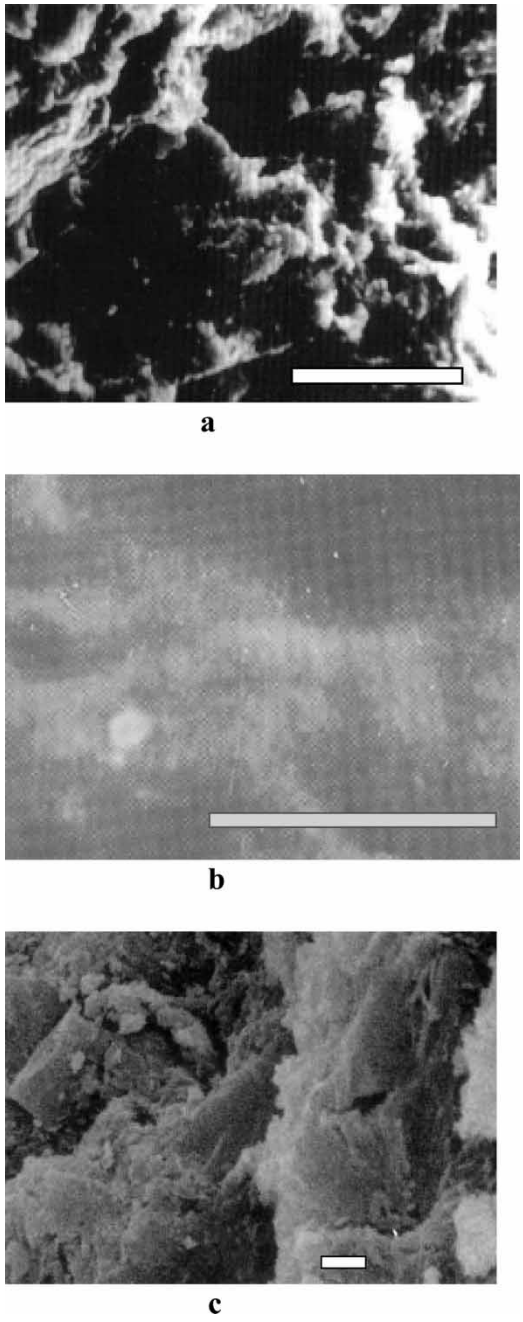

Figure 4. SEM micrographs of ceramic membranes prepared with powders of particle sizes $d_p = 100\ \mu m$, treated at 900°C, (bar = 20 μm) (17) (a), and 1100°C, (bar = 20 μm) (17) (b) and $d_p = 500\ \mu m$, treated at 800°C, during 2 hours (bar = 1 μm) (c).

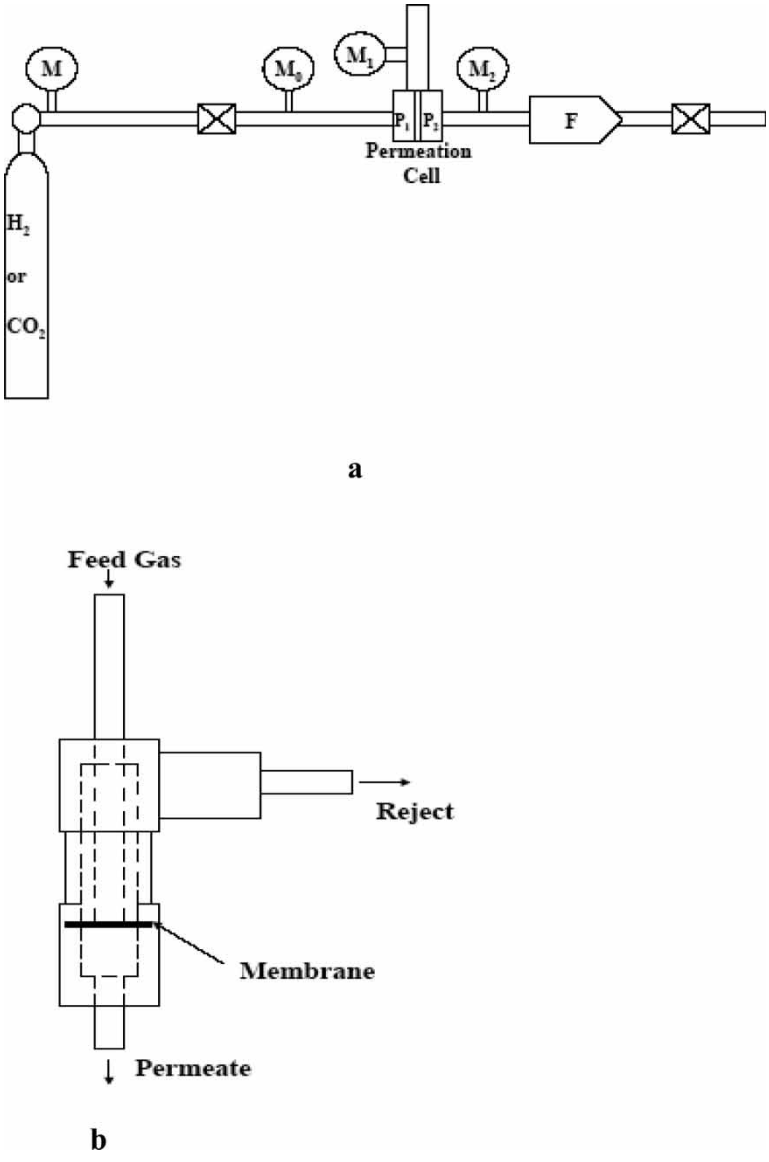

Figure 5. Diagrams of: the permeation test facility (a) and the permeation cell (b).

flux meters, and pressure transducers. The permeation cell (Fig. 5b) was coupled with two, Taber Corporation, pressure transducers (M_1 and M_2) to measure P_1, the reject pressure, and P_2, the permeate pressure, in the range from 0 to 70 MPa. An Alltech mass flow meter (F) measured the flux (J) passing through the membrane. The range of magnitude of the pressure P_1

was from 0.39 to 0.81 MPa. The pressure P_2 oscillated around 0.35 MPa. The feed pressure (P_0) measured with the pressure transducer (M_0) fluctuated between 0.41 to 0.83 MPa. The span of magnitude of the reject flow was from 2.2×10^{-5} to $2.6 \times 10^{-5}\,m^3/s$.

The ceramic membrane wafers were affixed on the stainless steel tubing comprising the permeation cell with a Viton® o-ring. Possible leakage through the o-ring was tested with a stainless steel wafer that had the same dimensions as the ceramic membrane wafers.

The permeation test facility was coupled with a mass-chromatograph, to analyze the product stream. However, since we only tested pure gases it was not used for this study.

The Permeability [B] and Permeance [Π] were measured with this equipment, with the help of the Darcy Law (Equation A1).

RESULTS AND DISCUSSION

Mechanism of High Temperature Phase Transformation of Natural Zeolites

Natural zeolites are three-dimensional microporous crystalline silico-aluminates which are built from SiO_4, AlO_4 and FeO_4 tetrahedra (simplified as TO_4) linked in the corners, sharing all oxygen atoms (21–24). Consequently, for each T atom there are two oxygen atoms, since the tetracoordinated, Si^{4+}, Al^{3+}, and Fe^{3+} are bonded by oxygen bridges. Therefore, the tetrahedra are really composed of two oxygen atoms per T atom, i.e., SiO_2, AlO_2 and FeO_2. Consequently, the presence of tetracoordinated Al^{3+} and Fe^{3+} generates a negative charge that must be balanced by extra-framework cations (one per Al^{3+} and Fe^{3+}). The chemical composition of natural zeolites can be expressed as:

$$M_{x/n}[(T^{3+}O_2)_x(T^{4+}O_2)_y] \cdot zH_2O$$

where $M_{x/n}$ are the balancing cations (charge $+n$) compensating the charge from the T^{3+} atom in tetrahedral coordination and z is the water contained in the voids of the zeolite (22, 23). The balancing cations, for natural zeolites, are normally alkaline cations (Na^+ or K^+) or alkaline earth cations (Ca^{2+} or Mg^{2+}) which are located within the zeolite channels and cavities (18, 23). These cations can be exchanged giving the zeolite its ion-exchange property (18, 23).

The structure of clinoptilolite (HEU framework type (21, 25)) show three channels, one 8-MR channel along [100], with an access of 2.6 A × 4.7 A, two parallel channels along [001] one 8-MR with a window of access with 3.3 A × 4.6 A and a 10-MR with an access of 3.0 A × 7.6 A (21). In Fig. 1a (16) and Fig. 3 are reported XRD patterns of natural clinoptilolites, which

fairly well coincide with the standard pattern reported in the collection of XRD profiles for zeolites (25).

The first step during the zeolite thermal treatment is its dehydration. Some natural zeolites, such as, clinoptilolite can be heated to 300–400°C and completely dehydrated without loss of crystallinity (18, 26). Consequently, the XRD pattern reported in Fig. 1a will not suffer a big change up to about 400°C.

If the zeolite temperature is increased to more than 500°C, after the dehydration an amorphization process takes place, which affects the material up to about 900°C (Figs. 1b, 1c, and 1d). During high temperature thermal treatment, that is, from 500–1100°C, the framework Al^{3+} and Fe^{3+} are extracted from the tetrahedral sites (24). This extraction of Al^{3+} and Fe^{3+} from the zeolite lattice, produces the amorphization of the zeolite framework (18, 24). After the amorphization from 900 to 1100 a recrystallization process occurs. This consist of reestablishment of the Si-O-Si bonds after the zeolite framework collapses, forming dense structures such as crystalline silica and a compact aluminosilicate. In our case this was cristobalite (αSiO_2) and the feldspar albite (Fig. 1e) (17, 18).

During the amorphization and recrystallization processes a change in density (17) (Fig. 2) was observed. A sharp density variation was evident from 900 to 1100°C. This was caused by the sintering of the powders that form the wafers (17). The same result of the sintering process is revealed by the SEM micrographs (Figs. 4a and 4b). The sample treated at 800°C (Fig. 4a) showed pores in the range $10\,\mu m < d_v < 20\,\mu m$. However, the sample treated at 1100°C (Fig. 4b) was compact. The SEM micrograph shown in Fig. 4c, obtained with a larger magnification, illustrates the morphology of a transformed natural zeolite grain.

Mechanical Properties

The ceramic membrane, produced with particles of grain diameter (d_p) of 220, 340 and 500 μm and treated at 800°C during 1 hour and 700 and 800°C during 2 h, resisted a pressure difference ($\Delta P = P_1 - P_2$) of 15 MPa, inside the permeation cell facility (Fig. 5b). The compression strength (C.S.) was also tested with the help of the Carver Manual Hydraulic Press Model 3912. The results were C.S. $= 25 \pm 5$ MPa. This means that the produced zeolite based ceramic membranes have enough resistance to be used in filtration and also as supports for the preparation of asymmetric membranes.

Estimation of Relation between Zeolite Particle Size and Membrane Pore Diameter

The apparent density (ρ_A) was considered as the mass density of a porous membrane and the real density (ρ_R) was the mass density of a compact

membrane, i.e, a membrane without porosity (in our case the membrane sintered at 1100°C (17)). With the help of the estimated porosity of the membranes (ε) it was possible to approximately calculate the membrane pore diameters (d_v), knowing the average particle diameters (d_p) used for the production of these membranes. If d_p is the particle diameter and d_v is the pore diameter of the membrane, then it is possible to propose a relation resembling the relations between sphere diameter and cell parameter in close packed structures (27):

$$d_v \approx \alpha d_p \tag{1}$$

where α is an adimensional proportionality constant.

If it is considered that:

$$\rho_A = \frac{m}{V_A} \quad \text{and} \quad \rho_R = \frac{m}{V_R}$$

where m is the mass of membrane included in the apparent volume V_A and the real volume V_R respectively, it can be shown that:

$$V_A \approx (1+\alpha)^3 V_R$$

Consequently with the help of Equation (A6 from the appendix) we obtain:

$$\varepsilon = 1 - \frac{1}{(1+\alpha)^3} \tag{2}$$

The estimated porosities of different porous membranes, obtained with the ceramic technique, are reported in Table 5. The porosity was calculated with help of Equation A6, the real membrane density was estimated as that corresponding to the membrane prepared at 1100°C. The other membranes were considered porous (17). This criterion was conceived with the help of wafer density measurements and a SEM study. With the help of Equations (1) and (2), the membrane pore diameter of the porous membrane synthesized for the present study were estimated Table 6.

Table 5. Estimated membrane porosity (ε)

Particle diameter d_p[μm]	Sample isothermal treatment temperature [°C]	Treatment isothermal time [hour]	ρ [g/cm^3]	ε
50–100	500	1	1.42 ± 0.03	0.36
50–100	600	1	1.42 ± 0.03	0.36
50–100	700	1	1.42 ± 0.03	0.36
50–100	800	1	1.50 ± 0.03	0.32
50–100	900	1	1.90 ± 0.03	0.14
50–100	1000	1	2.10 ± 0.03	0.05
50–100	1100	1	2.20 ± 0.03	0.00

Table 6. Estimated membrane pore diameters

Sample d_p [μm]	Sample isothermal treatment temperature [°C]	Sample isothermal treatment time [hour]	α	d_v [μm]
220	700	2	0.158	35
340	700	2	0.158	54
500	700	2	0.158	79
220	800	1	0.164	36
500	800	1	0.164	82
340	800	2	0.167	57
500	800	2	0.167	84

Permeation Test of Hydrogen and Carbon Dioxide in Clinoptilolite Based Ceramic Membranes

Gas transport mechanisms in porous and microporous membranes are laminar gas flow, Knudsen flow, surface diffusion, multilayer diffusion, capillary condensation and configurational diffusion (2, 9) (see appendix). In our case we will consider that configurational diffusion is not possible (12, 14–16), because during the wafer thermal treatment to obtain the ceramic membrane, the clinoptilolite framework collapsed. Besides, as was explained in the previous section, there were only macropores in our membranes. In addition, since, adsorption and capillary condensation in the surface of the membrane will be very weak, due to the relatively high temperature (300 K) and the somewhat low pressures (0.2–1.4 MPa) (9), it was also possible to exclude surface diffusion, multilayer diffusion and capillary condensation. Consequently, in our permeation test only Knudsen or Gaseous Flow could occur (2, 4, 5, 9).

Figures 6 to 9 show the results of different experiments of the permeation of H_2 and separately CO_2 in membranes obtained using different particle diameters, temperature and treatment time. In addition, in Table 7 are reported the Permeability [B] and Permeance [Π] of all the samples prepared in the current study. The Permeability [B] and Permeance [Π] were calculated with the help of the Darcy Law (Equation A1 in the appendix).

Membrane Pore Diameter Study

In Table 6 the estimated pore diameters of the membranes are reported, and these were in the range of 35–84 μm. Table 8 are reported the mean free path of H_2 and CO_2 at the temperatures and pressures of the permeation experiment. From these results it is evident that Knudsen flow was not possible since $d_v \gg \lambda$ (2, 4). Thus, the determining process in the present case is

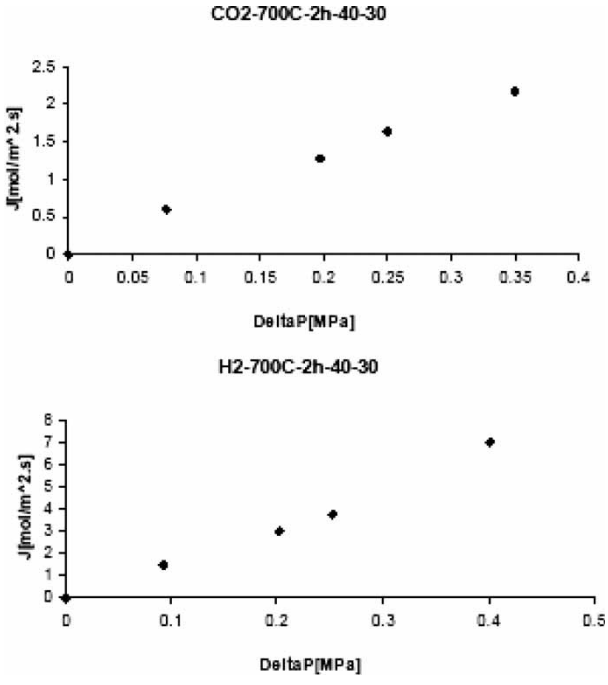

Figure 6. Permeation study of H_2 and CO_2 in a membrane produced by a thermal treatment at 700°C during 2 hours of a clinoptilolite powder of 500 μm of particle diameter.

gaseous laminar flow through the membrane pores. It is therefore feasible to apply the Darcy Law for gaseous laminar flow (13) (Equation A3). In addition, for the description of this flow it is necessary to employ the Carman-Kozeny relation (4, 13) (Equation A5), since the Hagen-Poiseuille equation is not suitable because our membrane was obtained by the sinterization of packed quasi-spherical particles (13).

Equations A3 and A5 were, at that time, used to measure the membrane pore diameter (d_v) (Table 9). The results coincided fairly well with the values previously estimated (Table 6). The size of the pores in the ceramic zeolite based membranes were determined using the average grain diameter (d_p) of the clinoptilolite powder used as raw material. The membrane pore size could be easily controlled by the grain size of the original natural zeolite raw material up to 1–5 μm, decreasing the average grain diameter of the raw material since: $d_v \approx \alpha d_p$ and $\alpha \approx 0.16$.

We have then produced, with an available and low cost material, such as natural clinoptilolite, novel, inexpensive, high permeation rate macroporous membranes with considerable mechanical strength. These could be used at relatively high temperature up to 500°C. Since as they were produced at

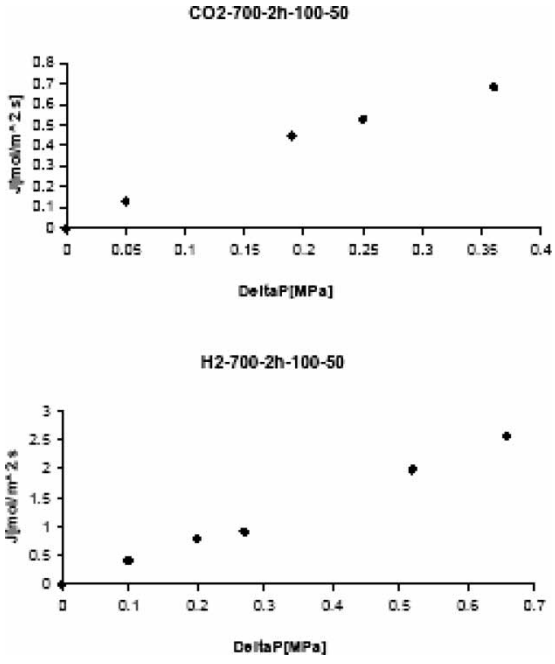

Figure 7. Permeation study of H_2 and CO_2 in a membrane produced by a thermal treatment at 700°C during 2 hours of a clinoptilolite powder of 220 μm of particle diameter.

700–800°C they will not suffer considerable further phase transformations or sinterization at 500°C. As far as the authors are aware there is no currently applications of this material in porous membrane production.

Hydrothermal Synthesis

Aluminosilicate zeolites are usually synthesized in hydrothermal conditions from solutions containing sodium hydroxide, sodium silicate, or sodium aluminate (28–30). From our previous experience, we know that it is possible to grow aluminosilicate zeolite crystals using aluminosilicates, as raw materials, under hydrothermal conditions, in a solution containing sodium hydroxide (30). However, the synthesis of an aluminosilicate zeolite over a membrane produced with the ceramic methodology applied here, in hydrothermal conditions, in a solution containing sodium hydroxide, caused the membrane amorphization and final dissolution. Therefore, we tried to synthesize an aluminophosphate zeolite (29) as $AlPO_4$-5 (31), over the zeolite porous ceramic membrane. The hydrothermal synthesis of this zeolite is carried out with an aluminophosphate gel (19). This almost certainly will not dissolve the membrane.

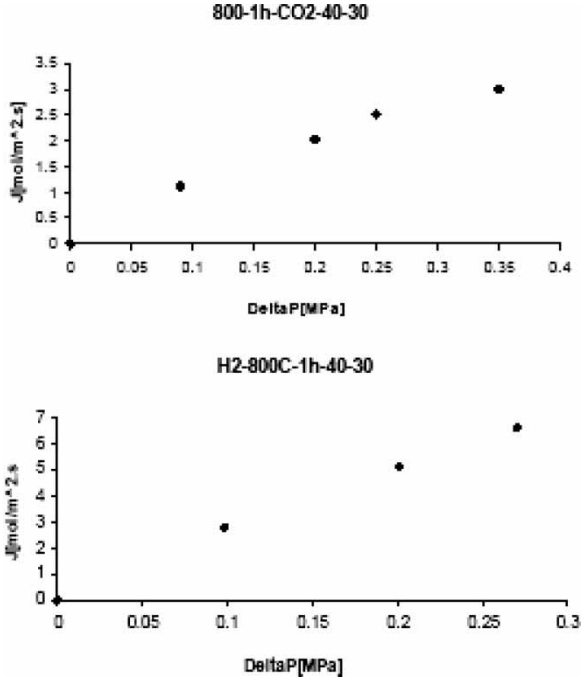

Figure 8. Permeation study of H_2 and CO_2 in a membrane produced by a thermal treatment at 800°C during 1 hours of a clinoptilolite powder of 500 μm of particle diameter.

Figure 10 reports the XRD pattern of the zeolite based ceramic membrane produced by sintering at 800°C a clinoptilolite powder ($d_p = 500\,\mu m$) for 2 hours, covered with an $AlPO_4$-5 molecular sieve produced with the methodology previously described (19). It is evident that the ceramic membrane, which is represented in the XRD pattern (Fig. 10) by the amorphous component of the XRD profile, was covered by the $AlPO_4$-5 molecular sieve, since the crystalline component of the obtained XRD pattern fairly well coincide with the standards reported in literature (25). Therefore, the porous support was coated with a zeolite layer hydrothermally formed, following the above described procedure (19). As a result a composite membrane, i.e., an $AlPO_4$-5 molecular sieve thin film-zeolite based ceramic, was produced.

The $AlPO_4$-5 molecular sieve has an AFI type framework, with a hexagonal cell, with idealized cell parameters a = 13.8 Å and c = 8.6 Å and a unidimensional 12 MR channel system with a window aperture of $7.3 \times 7.3\,Å^2$, parallel to the [001] direction (21). Subsequently, good separation factors could be obtained for some gas mixtures with this composite membrane (3, 9).

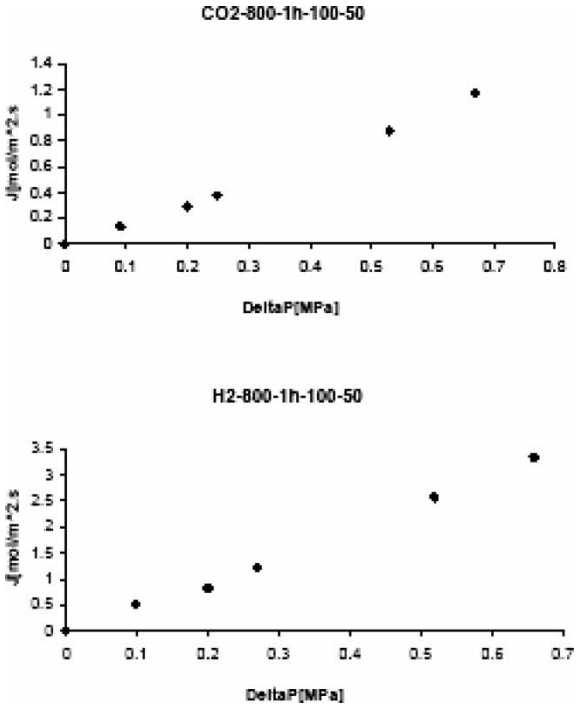

Figure 9. Permeation study of H_2 and CO_2 in a membrane produced by a thermal treatment at 800°C during 1 hours of a clinoptilolite powder of 220 μm of particle diameter.

The porous supports commonly used for the production of composite membranes are alumina, zirconia, porous glass, and stainless steel (1, 3, 9). Therefore the use of zeolite based porous ceramic membranes for this purpose is also a contribution of the present research.

CONCLUSIONS

New inexpensives, non-brittle macroporous ceramic zeolite based membranes with a significant permeation rate, were produced. This was accomplished by applying a ceramic methodology, consisting of the thermal transformation of natural clinoptilolite powders pressed to produce wafers. The XRD and SEM studies showed that the clinoptilolite amorphized at 600–900°C. A posterior recrystallization to a siliceous phase and a compact aluminosilicate phase occurs at 900–1150°C.

The permeation test allowed the measurement of the Permeability [B] and Permeance [Π] of H_2 and CO_2 with the help of the Darcy Law. The

Table 7. Hydrogen and carbon dioxide Permeability [B] and Permeance [Π] in the membranes

Sample d_p [μm]	Sample treatment temperature [°C]	Sample treatment time [hour]	Gas	$B \times 10^8$ [mol/m.s.Pa]	$\Pi \times 10^6$ [mol/m^2.s.Pa]
220	700	2	H_2	1.1	4.1
340	700	2	H_2	3.2	11.8
500	700	2	H_2	4.9	18.1
220	800	1	H_2	1.4	5.2
500	800	1	H_2	6.8	25.1
340	800	2	H_2	3.4	12.6
500	800	2	H_2	5.4	20.0
220	700	2	CO_2	0.5	1.8
340	700	2	CO_2	1.0	3.7
500	700	2	CO_2	1.7	6.3
220	800	1	CO_2	0.7	1.7
500	800	1	CO_2	2.4	8.9
340	800	2	CO_2	1.3	5.0
500	800	2	CO_2	2.4	8.9

Table 8. Mean free paths [λ] of Hydrogen and carbon monoxide at T = 300 K and different pressures

Pressure [MPa]	Gas	λ[nm]
0.2	H_2	55.4
0.4	H_2	27.7
0.6	H_2	18.4
0.8	H_2	13.9
1.0	H_2	11.1
1.2	H_2	9.2
1.4	H_2	7.9
0.2	CO_2	38.0.
0.4	CO_2	19.0
0.6	CO_2	12.7
0.8	CO_2	9.5
1.0	CO_2	7.6
1.2	CO_2	6.3
1.4	CO_2	5.4

Table 9. Hydrogen and carbon dioxide permeation [k] and membrane average pore diameter [d_v]

Sample d_p [μm]	Sample treatment temperature [°C]	Sample treatment time [hour]	Gas	$k \times 10^{12}$ [m^2]	d_v [μm]
220	700	2	H_2	4.4	32
340	700	2	H_2	12.7	58
500	700	2	H_2	19.4	69
220	800	1	H_2	5.5	38
500	800	1	H_2	27.0	83
340	800	2	H_2	13.5	59
500	800	2	H_2	21.4	74
220	700	2	CO_2	3.4	32
340	700	2	CO_2	6.8	45
500	700	2	CO_2	11.6	58
220	800	1	CO_2	5.1	35
500	800	1	CO_2	16.5	83
340	800	2	CO_2	9.2	62
500	800	2	CO_2	16.5	83

membrane pore sizes were calculated with the help of a simple model. Using this information it was possible to predict that the main regime in the membrane was laminar gas flow. Therefore the Carman-Kozeny equation for gaseous laminar flow, was applied. With the help of this equation the membrane pores sizes were measured. It was found that the porosity of the new porous ceramic zeolite based membranes can be

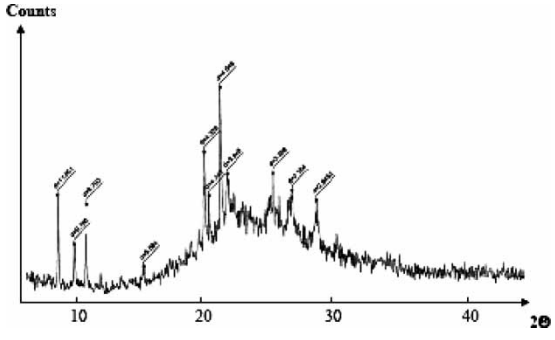

Figure 10. XRD pattern (counts per second [CPS] vs 2θ) of a ceramic membrane prepared with a clinoptilolite powder of $d_p = 500\,\mu m$ and treated at 800°C during 2 hours and later covered with an $AlPO_4$-5 molecular sieve. The interplanar distances (d in Å) of the $AlPO_4$-5 are reported for the more intense peaks (25).

easily controlled by the grain size of the original natural zeolite raw material up to 1–5 μm.

The membranes were also transformed by hydrothermal synthesis methodology to give materials covered with an $AlPO_4$-5 molecular sieve.

These new membranes were produced with natural clinoptilolite which is a low cost and available material. They have great potential in industrial filtration processes and also as support materials in composite membranes for gas separation.

APPENDIX

Transport Mechanisms in Porous Membranes

The permeation rate and selectivity of a porous inorganic membrane depends on its microstructure, i.e., pore size, and pore size distribution, tortuosity, permeating molecules and membrane pore walls interactions and permeating species mass and size (3–5).

In the course of the transport of gases through porous and microporous membranes, when pressure is the driving force of the process, the gaseous molecules will be transported from the high pressure to the low pressure side of the membrane. This transport process follows the Darcy Law (4, 13):

$$J = B\left(\frac{\Delta P}{l}\right) = \Pi\,\Delta P \tag{A1}$$

$$J = \frac{QVm}{A}$$

$$\Pi = \frac{B}{l} \tag{A2}$$

During the transport of gases through porous membranes, various mechanisms can take place depending on the temperature, pressure, and membrane pore diameters. Gaseous laminar flow can occur in wide pores, Knudsen flow in narrower pores, as well as surface diffusion, multilayer diffusion, and capillary condensation (2, 4).

Darcy Law for gaseous laminar flow is described by the following equation (13):

$$Q = \left(\frac{k}{\mu}\right) * A * \left(\frac{\Delta P}{l}\right) \tag{A3}$$

where

$$B = \frac{kV_m}{\mu} \tag{A4}$$

For the description of this flow, the Carman-Kozeny equation (4,13) can be employed, in the present case, because, the Hagen-Poiseuille equation is not valid, since, the membrane is inorganic, obtained by the sinterization of packed quasi-spherical particles.

The Carman-Kozeny equation for the permeability factor for a membrane formulated with pressed spherical particles is (13):

$$k = \frac{\varepsilon\, d_v^2}{16C} \tag{A5}$$

where (13):

$$\varepsilon = 1 - \frac{\rho_A}{\rho_R} \tag{A6}$$

Therefore:

$$k \approx \frac{\varepsilon\, d_v^2}{77} \tag{A7}$$

As the membrane pore dimensions decrease, or the mean free path of the molecules increase, the permeating particles tend to collide more with the pore walls than among themselves (12). The Knudsen flow regime is then established. In this case the expression for the permeation flux across the membrane is given by (2):

$$J = \left(\frac{G}{(2MRT)^{1/2}}\right) * \left(\frac{\Delta P}{l}\right) \tag{A8}$$

In the case of microporous materials, specifically zeolites, configurational diffusion is the term coined to describe molecular transport, it is characterized by very small diffusivities (10^{-8} to $10^{-14}\,cm^2/s$), a strong dependence on the size and shape of guest molecules, high activation energies ($10-100\,kJ/mol$) and a strong concentration dependence (15, 16). Mass transport in microporous media takes place in an adsorbed phase. When a molecule diffuses inside a zeolite channel, it becomes attracted to and repelled by different interactions, such as the dispersion energy, repulsion energy, polarization energy, field dipole energy, field gradient quadrupole, sorbate-sorbate interactions, and the acid-base interaction with the active site if the zeolite contains hydroxyl bridge groups (12, 15, 16). Consequently this transport can be pictured as an activated molecular hopping between fixed sites (12, 15, 16). Therefore, during the transport of gases through microporous membranes both diffusion between localized adsorption sites and the activated gas translation diffusion will contribute to the overall process (9, 12, 15).

The diffusion coefficient, in the case of mobile adsorption, for the transport of molecules in zeolite cavities and channels is (15):

$$\mathrm{D_m} = (1/2)[(\mathrm{RT}/\pi\mathrm{M})^{1/2}]\,\mathrm{L}\exp(-\mathrm{E_a}/\mathrm{RT}) \tag{A9}$$

The diffusion coefficient, in the case of localized adsorption, for the transport of molecules in zeolite cavities and channels is (15):

$$D_{\mathrm{l}} = \nu\, \mathrm{L} \exp(-\mathrm{E_a}/\mathrm{RT}) \qquad \text{(A10)}$$

NOMENCLATURE

A	effective membrane area [m^2]
B	Permeability [mol/m s Pa]
$C = 4.8 \pm 0.3$	Carman-Kozeny constant
d_p	average grain diameter [mm]
D_{m}	diffusion coefficient in the case of mobile adsorption [m^2/s]
D_{l}	diffusion coefficient in the case of localized adsorption [m^2/s]
$\mathrm{E_a}$	activation energy of the diffusion process [KJ/mol]
G	geometrical factor [m]
J	molar gas flow [mol/m^2 s]
k	permeation factor [m^2]
l	membrane thickness [m]
d_v	membrane pore diameter [μm]
L	jump distance between adsorption sites [m].
M	molecular weight of the gaseous permeating species [Kg/mol]
$\Delta P = \mathrm{P_1} - \mathrm{P_2}$	trans-membrane pressure [Pa],
Q	gas filtrate flux [m^3/s],
R	gas constant (J/kmolK)
T	temperature (K)
Vm	molar volume of the flowing gas [m^3/mol]

Greek Symbols

ε	membrane porosity
Π	gas permeance [mol/m^2 s Pa].
ρ_{A}	apparent membrane density [g/cm^3]
ρ_{R}	real membrane density [g/cm^3]
μ	dynamic viscosity of the gas [Pa.s]

ACKNOWLEDGEMENTS

The authors gratefully recognize the financial support provided by NASA through the Grant Cooperative Agreement Number NAG10-335 and the 2003 and 2004 Faculty Summer Research Fellowships granted to Mr. W. del Valle

at the NASA-Kennedy Space Center. We would also like to acknowledge the support given by our colleagues from the NASA-Kennedy Space Center: Dr. Clyde Parrish, Dr. Dave Bartine, and Mr. Eduardo Lopez del Castillo. The authors gratefully acknowledge the collaboration of the University of Turabo engineering student, Mr. Francisco Cabrera. Finally, it is also necessary to express our recognition to the Materials Characterization Center at the Rio Piedras Campus of the University of Puerto Rico for the support offered to carry out the XRD, SEM, and EDAX study.

REFERENCES

1. Hsieh, H.P. (1996) *Inorganic Membranes for Separation and Reaction*; Membrane Science and Technology Series 3, Elsevier: Amsterdam.
2. Saracco, G. and Specchia, V. (1994) *Catalytic Inorganic-Membrane-Reactors: Present Experience and Future Opportunities*; Catalysis Reviews-S&E, 36, 305–384.
3. Morooka, S. and Kusakabe, K. (1999) Microporous inorganic membranes for gas separation. *MRS Bulletin*, 25–29.
4. Mulder, M. (1996) *Basic Principles of Membrane Technology*. Kluwer Academic Publishers: Dordrecht, The Netherlands.
5. Baker, R.W. (2004) *Membrane Technology and Applications*; Wiley: New York.
6. Goosen, M.F.A., Sablani, S.S., and Roque-Malherbe, R. (2005) Membrane Fouling: Recent Strategies and Methodologies for its Minimization. In *Handbook of Membrane Separations: Chemical, Pharmaceutical, and Biotechnological Applications*; Pabby, A.K., Sastre, A.N.H. and Rizvi, S.S., eds.; Marcel Dekker: New York (In Press).
7. Saracco, G., Neomagus, H.W.J.P., Versteeg, G.F., and Swaaij, W.P.M. (1999) High-temperature membrane reactors: Potential and problems. *Chemical Engineering Science*, 54: 1997–2017.
8. Sankar, N. and Tsapatsis, M. (2003) In *Handbook of Zeolite Science and Technology*; Auerbach, S., Carrado, K.A. and Dutta, P.K., eds.; Marcell Dekker: New York, 867–919.
9. Burggraaf, A.J. (1999) Single gas permeation of thin zeolite (MFI) membranes: Theory and analysis of experimental observations. *Journal of Membrane Science*, 155: 45–65.
10. Vankelecom, I.F.J. (2002) Polymeric membranes in catalytic reactors. *Chem. Rev.*, 102: 3779–3810.
11. Boissiere, C., Martines, M.A.U., Kooyman, P.J., et al. (2003) Ultrafiltration membrane made with mesoporous MSU-X, silica. *Chem. Mater.*, 15: 460–463.
12. Xiao, J. and Wei, J. (1992) Diffusion mechanism of hydrocarbons in zeolites-I. *Chem. Eng. Science*, 47: 1123–1141.
13. Mauran, S., Rigaud, L., and Coudeville, O. (2001) Application of the Carman-Kozeny correlation to a high-porosity anisotropic consolidated medium: The compressed expanded natural graphite. *Transport in Porous Media*, 43: 355–376.
14. Krishna, R. (2003) Modeling issues in zeolite applications. In *Handbook of Zeolite Science and Technology*; Auerbach, S., Carrado, K.A. and Dutta, P.K., eds.; Marcell Dekker Inc.: New York, 1105–1139.

15. Roque-Malherbe, R., Wendelbo, R., Mifsud, A., and Corma, A. (1995) Diffusion of aromatic hydrocarbons in H-ZSM-5, H-Beta and H-MCM-22 zeolites. *J. Phys. Chem.*, 99: 14064–14071.
16. Karger, J., Vasenkow, S., and Auerbach, S.M. (2003) Diffusion in zeolites. In *Handbook of Zeolite Science and Technology*; Auerbach, S., Carrado, K.A. and Dutta, P.K., eds.; Marcell Dekker Inc.: New York, 341–422.
17. Hernández-Vélez, M., Raymond, O., Alvarado, A., et al. (1995) New materials obtained from high temperature phase transformations of natural zeolites. *J. Mat. Sci. Letters*, 14: 1653–1656.
18. Roque-Malherbe, R. (2001) Applications of natural zeolites in pollution abatement and industry. In *Handbook of Surfaces and Interfaces of Materials*; Nalwa, H.S., ed.; Academic Press: New York; Vol. 5, 495–522.
19. Robson, H. (2001) *Verified Synthesis of Zeolitic Materials*, 2nd Ed.; Elsevier: Amsterdam.
20. Semmens, M.J. (1984) *Cation-Exchange Properties of Natural Zeolites, in Zeo-Agriculture*; Pond, W.G. and Mumpton, F.A., eds.; Westview, Boulder, CO, USA, 45–54.
21. Baerlocher, Ch., Meier, W.M., and Olson, D.M. (2001) *Atlas of Zeolite Framework Types,* 5thEd.; Elsevier: Amsterdam.
22. Marquez-Linares, F. and Roque-Malherbe, R. (2003) Zeolites. Part 1. Structural features, synthesis, modification and characterization. *Facets-IUMRS Journal*, 2: 14–17.
23. Tsisihvili, G.V.T., Andronikashvili, T.G., Kirov, G.N., and Filizova, L.D. (1992) *Natural Zeolites*; Ellis Horwood: New York.
24. Roque-Malherbe, R., Diaz-Aguila, C., Reguera-Ruiz, E., et al. (1990) The state of iron in natural zeolites: A Mössbauer study. *Zeolites*, 10: 685–689.
25. Treacy, M.M.J. and Higgins, J.B. (2001) *Collection of Simulated XRD Powder Patterns for Zeolites,* 4thEd.; Elsevier: Amsterdam.
26. Bish, D.L. (1994) *Thermal properties of natural zeolites, in natural zeolites '93: occurrence, properties*; Ming, D.W. and Mumpton, F.A., eds. Interantional Committee on Natural Zeolites; Brockport, New York, 259–269.
27. Kasap, S.O. (2002) *Principles of Electronic Materials,* 2ndEd.; McGraw-Hill Higher Education: New York.
28. Barrer, R.M. (1982) *Hydrothermal Chemistry of Zeolites*; Academic Press: London.
29. Soler-Illia, G.J., Sanchez, C., Lebeau, B., and Patarin, J. (2002) Chemical strategies to design textured materials: from microporous and mesoporous oxides to nnonetworks and hierarchical structures. *Chem. Rev.*, 102: 4093–4138.
30. de las Pozas, C., Díaz-Quintanilla, D., Pérez-Pariente, J., et al. (1989) Hydrothermal transformation of natural clinoptilolite to zeolite Y and P. *Zeolites*, 9: 33–39.
31. Roque-Malherbe, R., López-Cordero, R., González-Morales, J.A., et al. (1993) A comparative study of MeAPO molecular sieves with AFI structure type. *Zeolites*, 13: 481–484.